Coulomb Corrections in Quasielastic Scattering off Heavy Nuclei

Andreas Aste

Department of Physics and Astronomy
Theory Division
University of Basel, Switzerland

Workshop on Precision ElectroWeak Interactions
The College of William & Mary
Thomas Jefferson National Accelerator Facility
Williamsburg, Virginia, August 16, 2005)

Overview

- Introduction
  - Basic remarks on quasielastic scattering
  - Failure of the plane wave Born approximation
- Coulomb distortion of electron wave functions
  - Classical considerations
  - Semiclassical description:
    * Wave front distortion (eikonal approximation)
    * Focusing
  - Effective momentum approximation (EMA)
- Exact calculations
  - Properties of exact continuum wave functions
  - Properties of the exact electron current
  - Comparison of exact calculations and EMA
- Conclusions

Long range Coulomb force

Problem:
The plane wave Born approximation (one photon exchange) may become inadequate for processes where heavy nuclei are involved.

- Charged particles are subject to virtual radiative corrections which are related to the long-range Coulomb forces

  $\longrightarrow$ exchange of many soft photons.

- The relevant expansion parameter αZ for perturbation theory is not small (e.g. $\alpha Z \simeq 0.6$ for lead, where Z=82).

  Example:

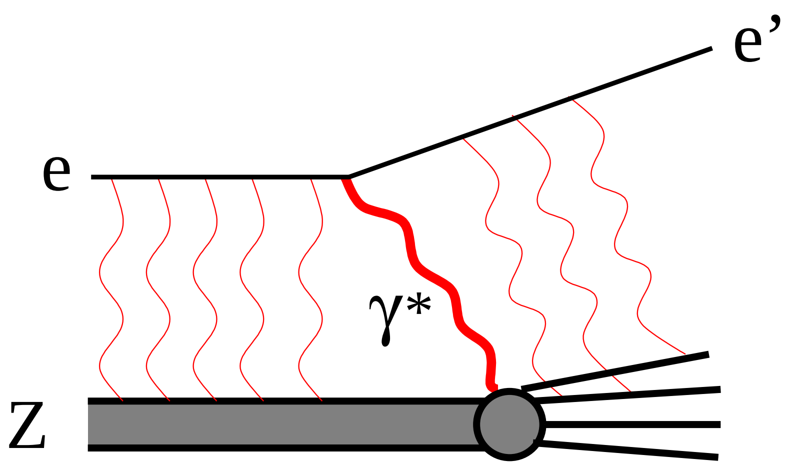

Inelastic scattering on a heavy nucleus with charge Z.

Quasielastic (e,e') scattering

Electron scattering is the main tool to explore the structure of nuclei. Nucleon knockout reactions (e.g., (e,e'p)) provide a powerful probe of several properties of the nucleons inside the nucleus. The transparency of the nuclear volume with respect to electrons makes it possible to study the entire nuclear volume.

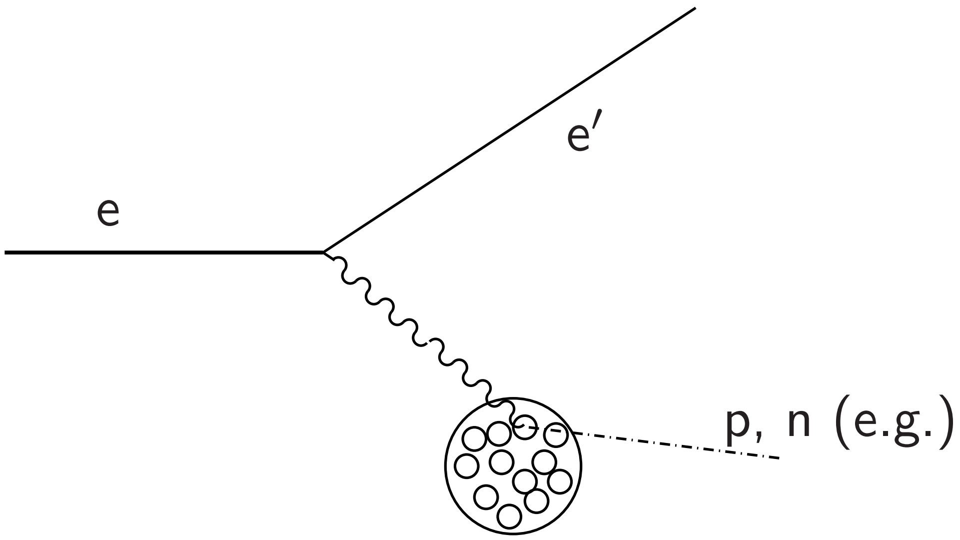

Inclusive (e,e') scattering (where only the final electron is observed) provides information about

- the nuclear Fermi momentum (width of the quasielastic peak)
- the high-momentum components of nucleon wave functions (tail of the quasielastic peak)
- modifications of the nucleon form factors inside a nucleus
- information about infinite nuclear matter by extrapolation $A \to \infty$.

Quasielastic peak

For electron scattering on a proton at rest, we obtain from four momentum conservation

$$-Q^2 = (k_i - k_f)^2 = (p_f - p_i)^2 = 2m_p^2 - 2m_p E_f,$$

and therefore

$$\omega = (E_f - m_p) = \frac{Q^2}{2m_p}.$$

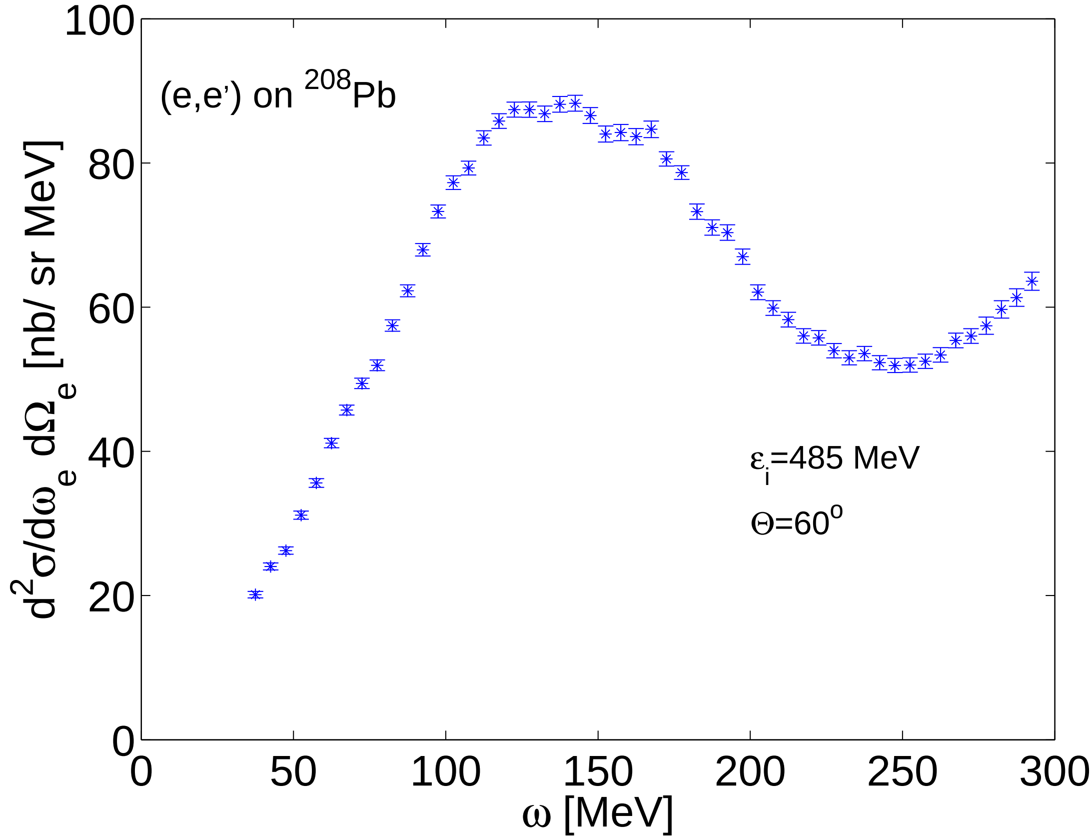

Quasielastic scattering on ^{208}Pb with initial electron energy $\epsilon_i = 485$ MeV, $\omega_{Peak} = 100$ MeV.

A. Zghiche *et al.*, Nucl. Phys. **A572** (1994) 513.

Knockout cross section

The differential cross section for nucleon knockout is given by

$$\frac{d^4\sigma}{d\epsilon_f d\Omega_f dE_f d\Omega_f} =$$

$$4\alpha^2\epsilon_f^2 E_F P_F \delta(\epsilon_i + E_A - \epsilon_f - E_F - E_{A-1}) \sum |W_{if}|^2,$$

with the matrix element

$$W_{if} = \int d^3x \int d^3y \int \frac{d^3q}{(2\pi)^2} j_\mu^e(\vec{x}) \frac{e^{-i\vec{q}(\vec{x}-\vec{y})}}{q_\mu^2} J_N^\mu(\vec{y}),$$

where $J_N^\mu(\vec{y})$ is the nucleon current obtained from some suitable model and q_μ^2 the virtuality of the exchanged photon.

In the plane wave Born approximation, the electron current is given by

$$j^\mu(\vec{x}) = \bar{u}_{s_f}(\vec{k}_f)\gamma^\mu u_{s_i}(\vec{k}_i)e^{i\vec{k}_i\vec{r}-i\vec{k}_f\vec{r}},$$

where the u_{s_i}, u_{s_f} are the initial/final state plane wave electron spinors corresponding to the initial/final electron momentum $k_{i,f}$ and initial/final spin $s_{i,f}$.

However, the Coulomb potential of nuclei distorts the electron wave functions such that the plane wave Born approximation becomes inaccurate.

Distortion of the wave front: eikonal approximation

Highly relativistic electron in a potential V with momentum $\vec{k}$: $m \ll V \ll |\vec{k}|$

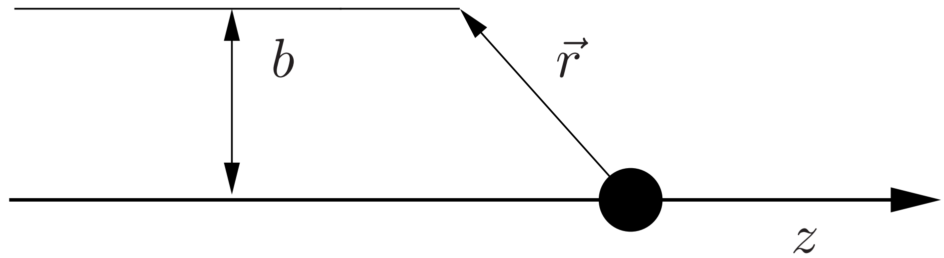

Classical motivation: Highly energetic electron incident in z-direction is moving along a straight line with impact parameter b.

The momentum $k = |\vec{k}|$ is enhanced due to the attractive nucleus

$$(E - V)^2 = \vec{k}^2 + m^2 \rightarrow k = E - V \text{ for } m \sim 0.$$

The momentum change can be taken into account by modifying the plane wave describing the electron by an eikonal phase $\chi_i(\vec{r})$

$$e^{i\vec{k}_i\vec{r}} \rightarrow e^{i\vec{k}_i\vec{r}+i\chi_i(\vec{r})},$$

where

$$\chi_i(\vec{r}) = -\int_{-\infty}^{z} V(x, y, z')\, dz'.$$

Reason:

$$\frac{\partial_z}{i} e^{i\vec{k}_i\vec{r}+i\chi_i(\vec{r})} = (k_z^i - V(\vec{r}))e^{i\vec{k}_i\vec{r}+i\chi_i(\vec{r})}$$

Eikonal distorted wave Born approximation

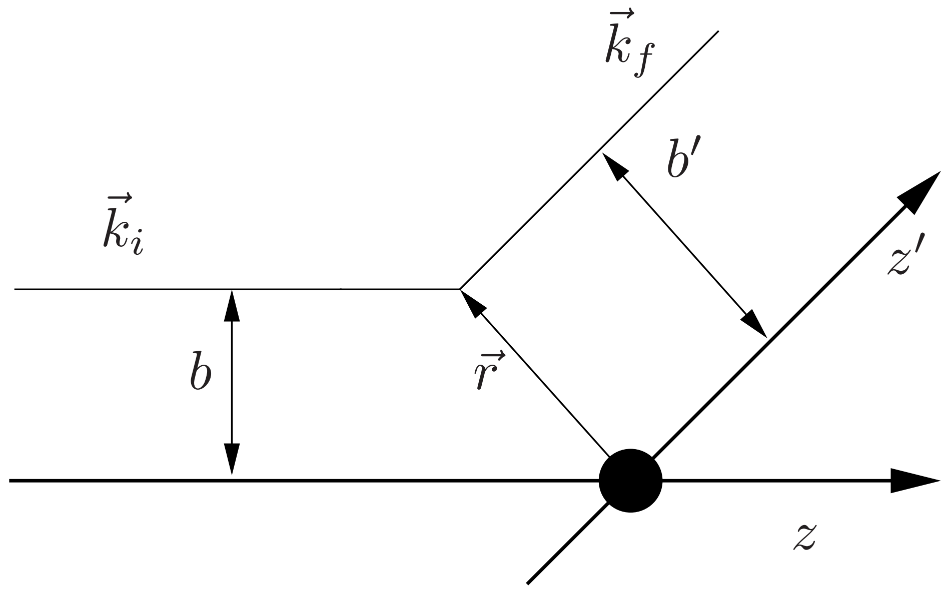

The final state wave function is modified analogously by replacing

$$e^{i\vec{k}_f\vec{r}} \longrightarrow e^{i\vec{k}_f\vec{r}-i\chi_f(\vec{r})},$$

where

$$\chi_f(\vec{r}) = -\int_0^\infty V(\vec{r}+\hat{k}_f s')ds'.$$

In the eikonal distorted wave born approximation (EDWBA), the electron current

$$j^\mu(\vec{r},t) = \bar{u}_{s_f}(\vec{k}_f)\gamma^\mu u_{s_i}(\vec{k}_i)e^{i\vec{k}_i\vec{r}-i\vec{k}_f\vec{r}-i(\epsilon_i-\epsilon_f)t}$$

is replaced by an improved expression

$$j^\mu(\vec{r},t) = \bar{u}_{s_f}(\vec{k}_f)\gamma^\mu u_{s_i}(\vec{k}_i)e^{i\vec{k}_i\vec{r}-i\vec{k}_f\vec{r}-i(\epsilon_i-\epsilon_f)t}e^{i\chi(\vec{r})},$$

where $\chi(\vec{r}) = \chi_i(\vec{r}) + \chi_f(\vec{r})$.

Focusing

The attractive electrostatic potential of the nucleus leads to a focusing of the electron wave in the nuclear vicinity.

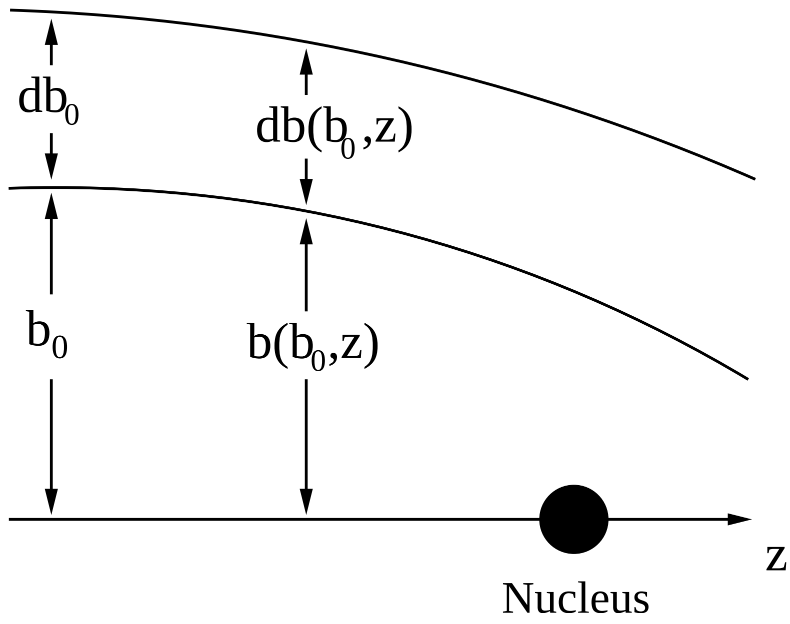

A classical calculation leads to the same approximate result as an approximate quantum mechanical calculation for the focusing in the center of the nucleus: The amplitude of the electron wave $(\bar{\Psi}_{i,f}\gamma^0\Psi_{i,f})^{1/2}$ in the nuclear center $(r=0)$ is enhanced by a factor

$$k_{\text{eff}}^{i,f}/k, \quad k_{\text{eff}}^{i,f} = k^{i,f} - V(0).$$

Example: An electron with initial energy/momentum 300 MeV(/c), energy transfer $\omega = 100$ Mev. Modification of the cross section due to focusing by a Pb nucleus ($V(0) \sim 25$ MeV)
$\sim (325/300)^2 \times (225/200)^2 = 1.49$.
N.B. $(319/300)^2 \times (219/200)^2 = 1.36$

Exact calculations show how the focusing is varying inside the nuclear volume.

Electron wave functions in a central electrostatic field

Dirac spinors describing states with definite angular momentum and parity can be decomposed into a radial and an angular part

$$\psi_\kappa^\mu = \begin{pmatrix} g_\kappa(r)\chi_\kappa^\mu(\hat{\mathbf{r}}) \\ if_\kappa(r)\chi_{-\kappa}^\mu(\hat{\mathbf{r}}) \end{pmatrix}$$

where the angular dependence is given by sperical harmonics

$$\chi_\kappa^\mu = \begin{pmatrix} \sqrt{\frac{j+\mu}{2j}} Y_{l,\mu-\frac{1}{2}} \\ \sqrt{\frac{j-\mu}{2j}} Y_{l,\mu+\frac{1}{2}} \end{pmatrix} \text{ for } \kappa < 0,$$

$$\chi_\kappa^\mu = \begin{pmatrix} -\sqrt{\frac{j-\mu+1}{2j+2}} Y_{l,\mu-\frac{1}{2}} \\ \sqrt{\frac{j+\mu+1}{2j+2}} Y_{l,\mu+\frac{1}{2}} \end{pmatrix} \text{ for } \kappa > 0,$$

where $\kappa = \pm 1, \pm 2, \ldots$ is related to j and l by

$$\kappa = l(l+1) - (j+\frac{1}{2})^2, \quad j = |\kappa| - \frac{1}{2}, \quad l = j + \frac{1}{2}\text{sgn}(\kappa).$$

The radial functions g and f fulfill the coupled differential equations

$$\frac{d}{dr}\begin{pmatrix} g_\kappa \\ f_\kappa \end{pmatrix} = \begin{pmatrix} -\frac{\kappa+1}{r} & E+m-V \\ -(E-m-V) & \frac{\kappa-1}{r} \end{pmatrix} \begin{pmatrix} g_\kappa \\ f_\kappa \end{pmatrix}.$$

Electron wave function in the electrostatic potential of ^{208}Pb

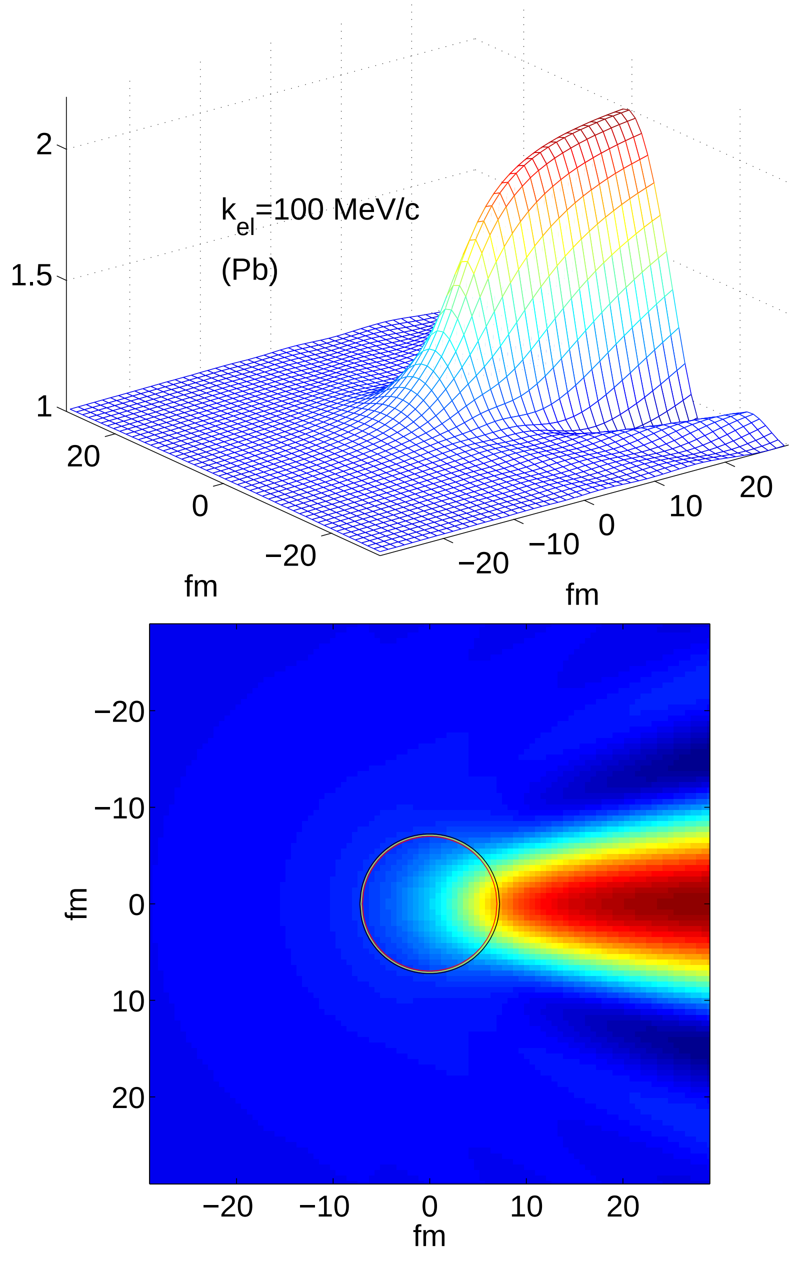

Surface and color plot of $(\bar{\Psi}\gamma^0\Psi)^{1/2}$ for an electron with energy 100 MeV incident on a point-like charge ($Z = 82$).

Electron wave function in the electrostatic potential of ^{208}Pb

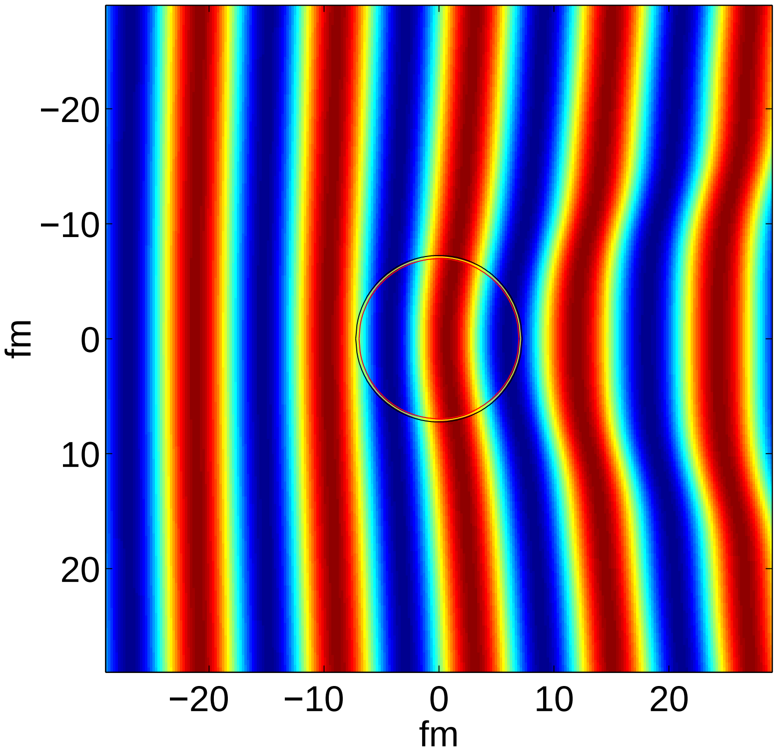

Visualization of the distortion of the wave front of the first (largest) spinor component ($\mathrm{Re}\,\psi^1/|\psi^1|$) for an electron with energy 100 MeV incident on a point-like charge ($Z = 82$).

Focusing of the wave function in the nuclear center (Pb, $V(0) = 25.7$ MeV)

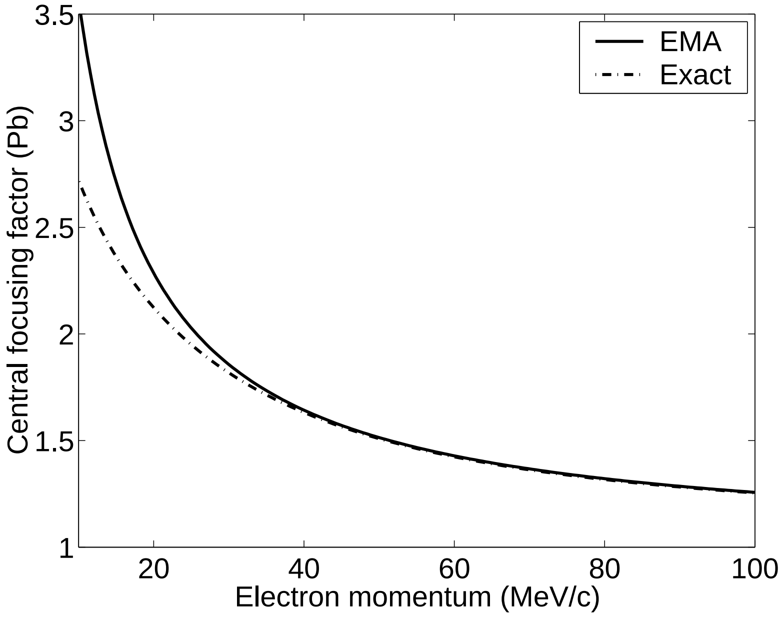

The prediction of the effective momentum approximation (EMA) that the amplitude of the electron wave function is enhanced by a factor of $(k - V(0))/k$ in the nuclear center, is very well fulfilled.

However, according to Lenz and Rosenfelder, we can expand

$$\psi_\tau = e^{\pm i\delta_{1/2}} \frac{k'}{k} e^{i\vec{k}'\vec{r}} [1 + g^{(1)}(a, b, \vec{k}', \vec{r}) + g^{(2)}(a, b, \vec{k}', \vec{r}) + \ldots] u_\tau,$$

$$k' = k + \frac{3\alpha Z}{2R}, \quad \delta_{1/2} = \alpha Z \left(\frac{4}{3} - \log 2kR \right) + b,$$

$$a = -\frac{\alpha Z}{6k' R^3}, \quad b = -\frac{3\alpha Z}{4k'^2 R^2},$$

with $\vec{k}'$ parallel to $\vec{k}$. These values enter the first-order term according to

$$g^{(1)} = ar^2 + iar^2 \vec{k}'\vec{r} \pm ib[(\vec{k}' \times \vec{r})^2 + 2i\vec{k}'\vec{r} - \vec{s}(\vec{k}' \times \vec{r})].$$

Focusing of the wave function in longitudinal direction

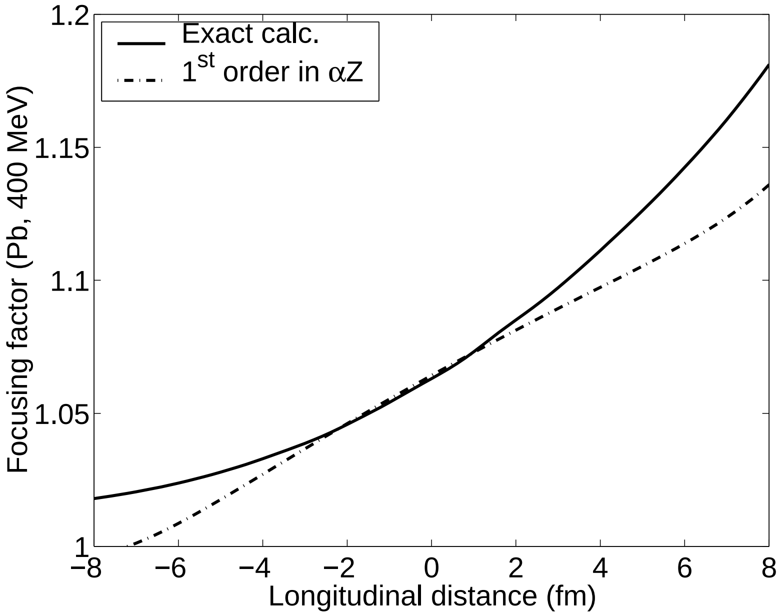

$$\psi_\tau = e^{\pm i\delta_{1/2}} \frac{k'}{k} e^{i\vec{k}'\vec{r}} [1 + g^{(1)}(a, b, \vec{k}', \vec{r}) + g^{(2)}(a, b, \vec{k}', \vec{r}) + \ldots] u_\tau,$$

$$k' = k + \frac{3\alpha Z}{2R}, \quad \delta_{1/2} = \alpha Z \left(\frac{4}{3} - \log 2kR \right) + b,$$

$$a = -\frac{\alpha Z}{6k' R^3}, \quad b = -\frac{3\alpha Z}{4k'^2 R^2},$$

$$g^{(1)} = ar^2 + iar^2 \vec{k}'\vec{r} \pm ib[(\vec{k}' \times \vec{r})^2 + 2i\vec{k}'\vec{r} - \vec{s}(\vec{k}' \times \vec{r})].$$

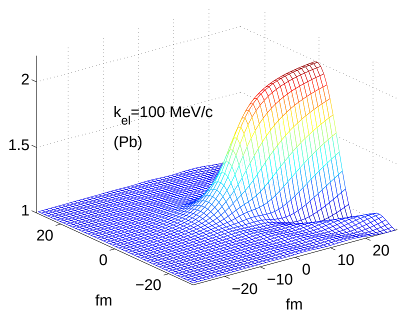

Focusing of the wave function in transverse direction

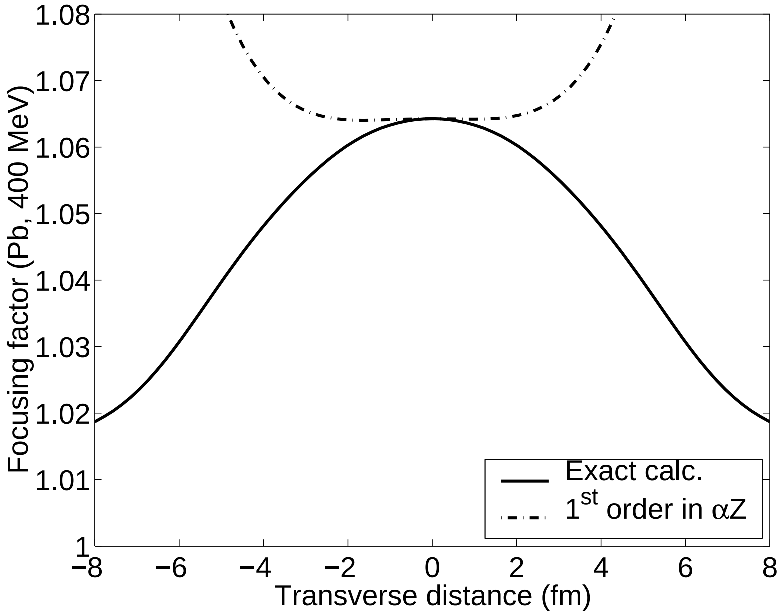

$$\psi_\tau = e^{\pm i\delta_{1/2}} \frac{k'}{k} e^{i\vec{k}'\vec{r}} [1 + g^{(1)}(a, b, \vec{k}', \vec{r}) + g^{(2)}(a, b, \vec{k}', \vec{r}) + \ldots] u_\tau ,$$

$$k' = k + \frac{3\alpha Z}{2R}, \quad \delta_{1/2} = \alpha Z \left(\frac{4}{3} - \log 2kR \right) + b,$$

$$a = -\frac{\alpha Z}{6k'R^3}, \quad b = -\frac{3\alpha Z}{4k'^2 R^2},$$

$$g^{(1)} = ar^2 + iar^2 \vec{k}'\vec{r} \pm ib[(\vec{k}' \times \vec{r})^2 + 2i\vec{k}'\vec{r} - \vec{s}(\vec{k}' \times \vec{r})].$$

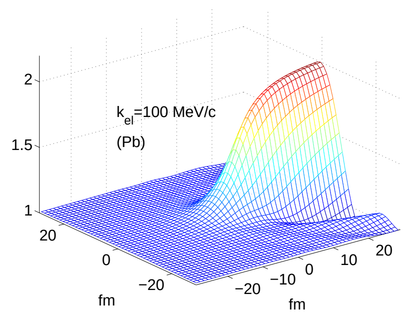

Wave lenght modification due to the electrostatic potential

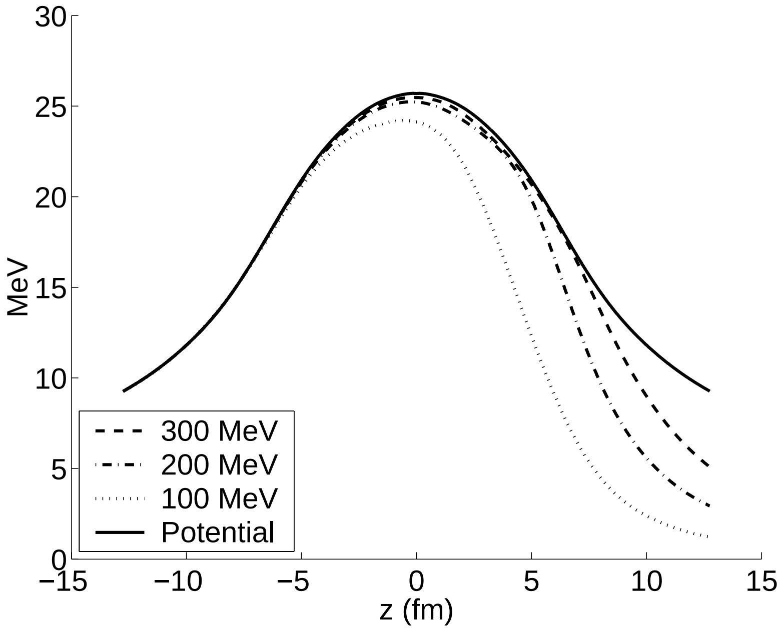

In order to check the quality of the eikonal approximation which modifies the (incoming) electron phase according to

$$\chi_i(\vec{r}) = -\int_{-\infty}^{z} V(x, y, z')dz' ,$$

one may calculate the phase of the first (large) component $\psi^1_{1/2}$ from the exact electron spinor along the z-axis, and extract the quantity χ_i^{ex} by setting

$$e^{ik_i z + i\chi_i^{ex}(z)} = \psi^1_{1/2}(z)/|\psi^1_{1/2}(z)|.$$

If the eikonal approximation were exact, then the derivative $\frac{d}{dz}\chi_i^{ex}(z)$ would be equal to the negative value of the electrostatic potential

$$\frac{d}{dz}\chi_i^{ex}(z) = -V(z).$$

Average focusing and average momentum

One is naturally lead to the idea to calculate an average focusing factor $\bar{f}$ defined by

$$\bar{f}^{\,2} = \frac{\int d^3r \bar{\psi}_\tau(\vec{r})\gamma^0\psi_\tau(\vec{r})\rho(r)}{\int d^3r\rho(r)},$$

where $\rho(r)$ is the nuclear matter density distribution ($\sim$ charge density profile of the nucleus for sufficiently large mass numbers $A > 20$).

For a typical electron energy of 400 MeV, one obtains $\bar{f} = 1.050$ for ^{208}Pb, corresponding to an effective potential value of -20.07 MeV (with a central potential depth of $V_0 = -25.7$ MeV).
For ^{40}Ca one obtains $-7.76\,/-10.4$ MeV.

Defining an effective potential value $\bar{V}$ by

$$\bar{V} = \frac{\int d^3r \bar{\psi}_\tau(\vec{r})\gamma^0\psi_\tau(\vec{r})\rho(r)V(r)}{\int d^3r \bar{\psi}_\tau(\vec{r})\gamma^0\psi_\tau(\vec{r})\rho(r)},$$

leads to the very similar values $\bar{V} = -20.12$ MeV for ^{208}Pb and $\bar{V} = -7.78$ MeV for ^{40}Ca.

This observation is a strong argument that both the focusing and the modification of the electron momentum inside the nucleus are well described by effective momenta corresponding to an effective potential $\sim 3V_0/4 \ldots 4V_0/5$.

Transition charge density

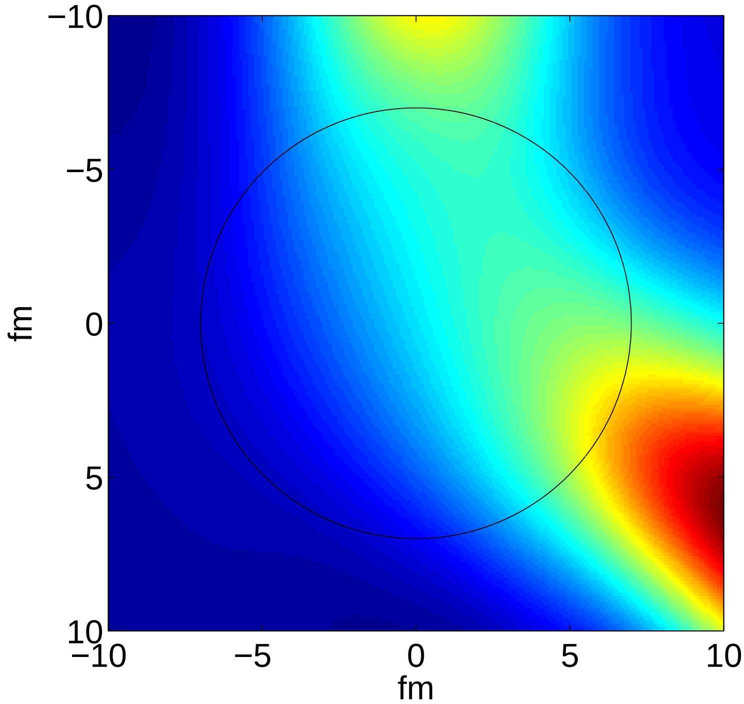

$\epsilon_i = 300$ MeV, $\epsilon_f = 200$ MeV, $\theta_e = 60^o$.

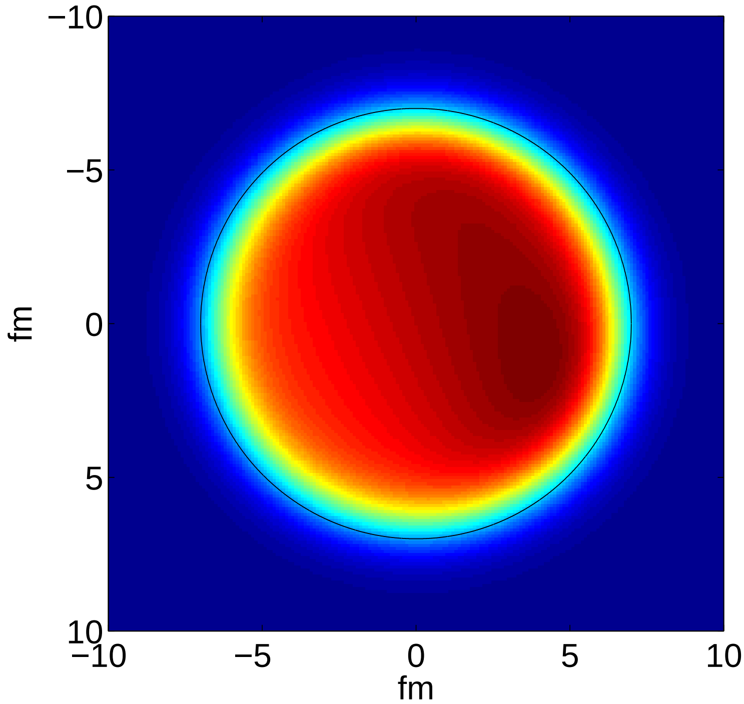

Transition charge density multiplied by Woods-Saxon profile.

Effective momentum approximation

The basic idea of the effective momentum approximation is to replace the plane wave part of the electron wave functions by

$$e^{i\vec{k}_{i,f}\vec{r}} \rightarrow \frac{k'_{i,f}}{k_{i,f}} e^{i\vec{k}'_{i,f}\vec{r}}.$$

The quasielastic scattering cross section is calculated by using the effective momenta $\vec{k}'_{i,f}$ instead of $\vec{k}_{i,f}$.
The cross section is multiplied additionally by a factor $(k'_i/k_i)^2$ which accounts for the focusing of the incoming electron wave in the nuclear center. The cross section is not multiplied by $(k'_f/k_f)^2$, because this factor is already contained in the artificially enhanced phase space factor of the outgoing electron.

The cross section for inclusive quasielastic electron scattering can also be written by the help of the total response function S_{total} as

$$\frac{d^2\sigma_{PWBA}}{d\Omega_f d\epsilon_f} = \sigma_{Mott} \times S_{total}(|\vec{q}|, \omega, \Theta_e), \tag{1}$$

where the Mott cross section is given by

$$\sigma_{Mott} = 4\alpha^2 \cos^2(\Theta_e/2)\epsilon_f^2/q_\mu^4. \tag{2}$$

The Mott cross section remains unchanged when it gets multiplied by the EMA focusing factors and the momentum transfer q_μ^4 is replaced by its corresponding effective value. Therefore, the EMA cross section can also be obtained from (1) by leaving the Mott cross section unchanged and by replacing $S_{total}(|\vec{q}|, \omega, \Theta_e)$ by the effective value $S_{total}(|\vec{k}'_i - \vec{k}'_f|, \omega, \Theta_e)$.

Simplification of the scattering matrix element

The DWBA transition amplitude for one-photon exchange in real space

$$\int d^3r_e d^3r_N \left\{\rho_e(\vec{r}_e)\rho_{if}(\vec{r}_N) - \vec{j}_e(\vec{r}_e)\vec{J}_{if}(\vec{r}_N)\right\} \frac{e^{i\omega r}}{|\vec{r}_e - \vec{r}_N|}$$

can be simplified according to Jörn Knoll (Nucl. Phys. **A223**, 1974, 462-476) by the help of an operator S

$$S = e^{i\vec{q}\vec{r}} \sum_{n=0} \left(\frac{2i\vec{q}\vec{\nabla} + \Delta}{\vec{q}^2 - \omega^2}\right)^n e^{-i\vec{q}\vec{r}}, \quad \vec{q} = \vec{k}_i - \vec{k}_f,$$

such that the transition amplitude can be expanded in a more convenient local form ($Q^2 = \vec{q}^2 - \omega^2$)

$$T_{if} = \frac{4\pi}{Q^2} \int d^3r \Big[\rho_{if}(\vec{r}) S \rho_e(\vec{r}) - \vec{J}_{if} S \vec{j}_e(\vec{r})\Big].$$

The single integral is limited to the region of the nucleus, where the nuclear current is relevant. The transition amplitude can be calculated therefore by numerical integration on a three-dimensional grid.

Focusing versus enhanced momentum transfer

Considering terms up to second order in the derivatives only one obtains for the operator S

$$S \approx e^{i\vec{q}\vec{r}} \left[1 + \frac{2i\vec{q}\vec{\nabla} + \Delta}{Q^2} - \frac{4(\vec{q}\vec{\nabla})^2}{(Q^2)^2} \right] e^{-i\vec{q}\vec{r}}$$

The gradient operator $\vec{\nabla}$ in probes mainly the distortion of the electron current due to the nuclear Coulomb potential.
A short calculation shows that ($\epsilon_{i,f} \gg m$)

$$\frac{Q'^2}{Q^2} = \frac{k'_i k'_f}{k_i k_f}, \tag{1}$$

where $Q'^2 = (\vec{k}'_i - \vec{k}'_f)^2 - \omega^2$ is the effective four-momentum transfer squared. When cross sections are calculated using the EMA, the enhanced photon propagator appearing in the matrix element cancels exactly the focusing effect of the initial and final state wave function.

A numerical analysis of the effect of the Knoll operator on the electron current shows that this is indeed also true for the DWBA to a relatively high degree of accuracy. However, this does not mean that effects are absent in the full calculation of transition matrix elements which lead to deviations between EMA and DWBA.

Knoll operator

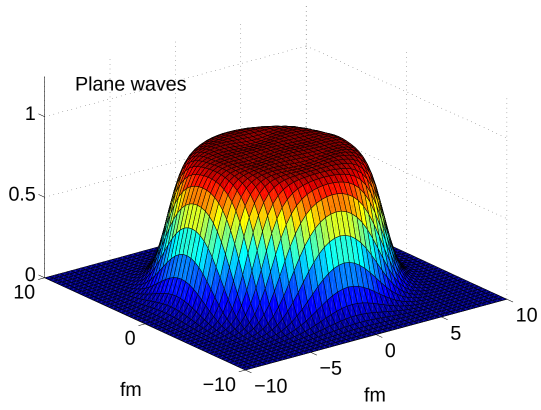

Electron charge density times Woods-Saxon profile: Plane waves. $k_i = 300$ MeV, $k_f = 200$ MeV, $\theta_e = 60^o$.

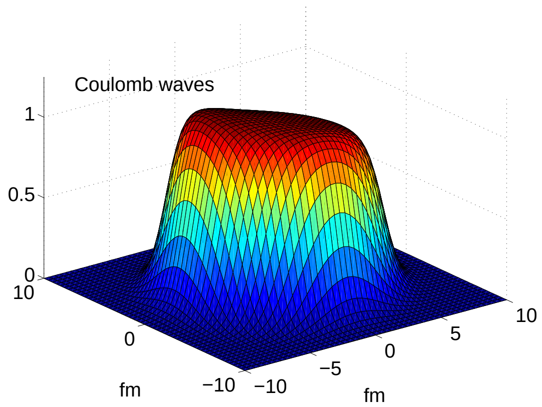

Coulomb waves: Charge density enhanced due to focusing.

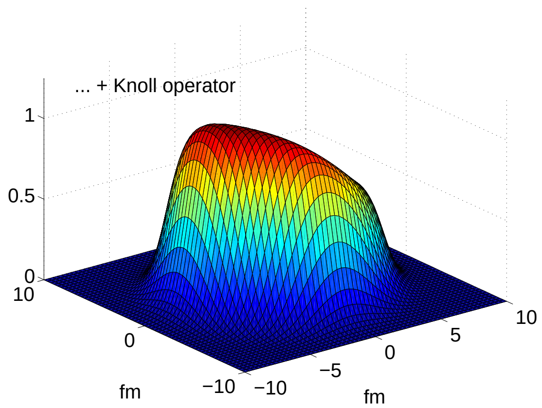

After applying the Knoll operator to the charge density.

Eikonal and EMA calculations revisited

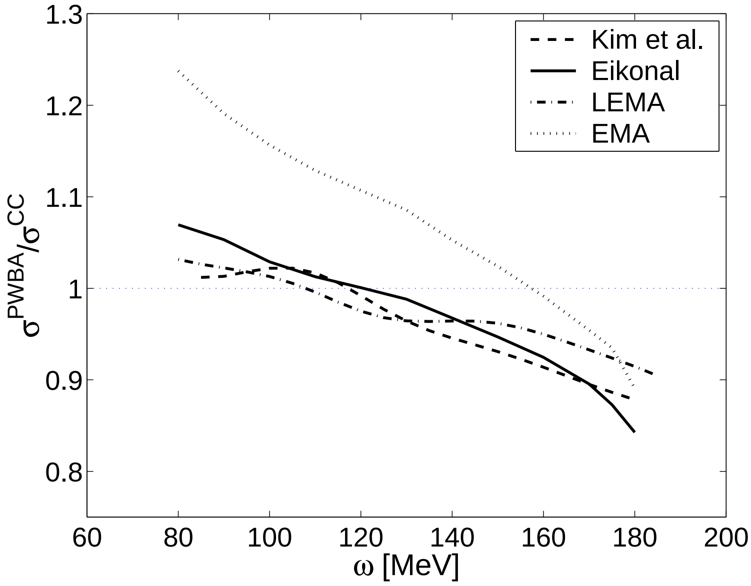

Old eikonal approximation calculation with overestimated focusing and EMA with central potential value.

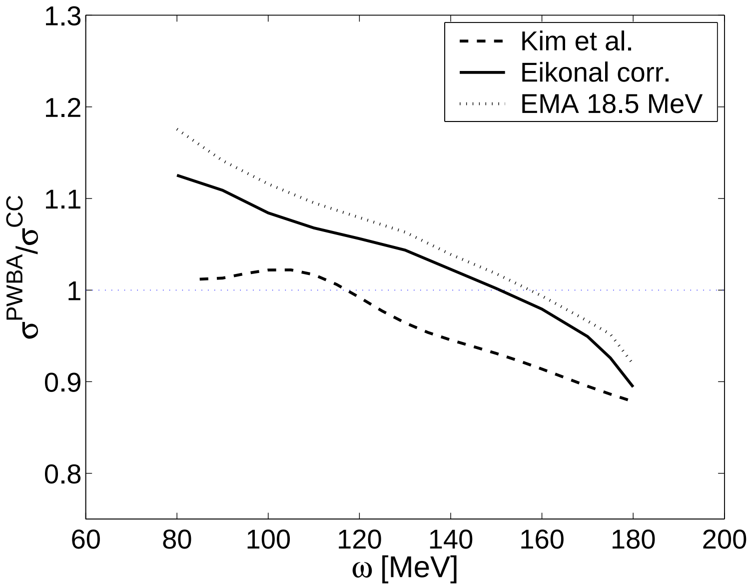

After approximate correction of the focusing and EMA with effective potential ~ 18.5 MeV.

Coupling to nuclear current

Preliminary calculations with

- harmonic oscillator wave functions for bound nucleon states and
- plane waves for final nucleon states

confirm the validity of an EMA-like description.

Bound states are characterized by

- quantum numbers (n, l, m)
- associated binding energies $E_B = V_0 - (N + \frac{3}{2})\hbar\omega_o$, $N = 2n + l - 2$, $\hbar\omega_o \sim 41\,\text{MeV}A^{-1/3}$
- the rms radius given by the equation $\langle nl|r^2|nl\rangle = x_o^2(N + \frac{3}{2})$, $x_o^2 = \hbar/m_n\omega_o$.

EMA-like behavior can be observed even for inclusive (e,e') scattering on filled shells (i.e. after summing over magnetic quantum numbers $m = -l...l$ for given energy and angular momentum $\sim N, l$) for initial electron energy > 400 MeV and $Q^2 > (400\,\text{MeV})^2$.

Exact match of DWBA and EMA can often be reached with 'optimized' effective potential $V_{\text{eff}} < 20$ MeV for individual shells. The difference between DWBA and EMA cross sections (for $V_{\text{eff}} = 20$ MeV) is typically in the range of $0... \pm 8\%$, and becomes smaller for growing momentum transfer and electron energies.

However:

Harmonic wave functions or plane waves provide a very poor description of the nucleon wave functions. Coulomb corrections may depend strongly on the nuclear model.

But:

Using plane waves for nucleons with 'wrong' energy, i.e. varying the energy of the outgoing nucleons by ± 20 MeV does not change the situation significantly: Absolute inclusive cross sections are changed, but the DWBA results still show an EMA-like behavior.

Filled shells (spherically symmetric configurations) still show an EMA-like behavior.

Therefore, one may conclude that the exact structure of the nuclear current is relevant for the calculation of absolute cross sections, but an EMA-like description can be found independently of the model used for the nucleus. Calculations with more realistic nucleon wave functions will follow in the forthcoming weeks in oder to clarify how the discrepancy between EMA and exact (DWBA) results can be described.

Conclusions

- The strong Coulomb field of heavy nuclei acts as a kind of lens on electrons. The effect of the lens is twofold:
  - Focusing of the electron wave function
  - Change of the electron momentum

  in the nuclear interior.
- Both the average momentum and the average focusing inside the nucleus can be described quite accurately by a common parameter (effective potential). The photon propagator cancels nearly exactly the focusing effect in the electron current (at least at high energies).
- The effective momentum approximation works very well for initial electron energies above 400 MeV and $Q^2 > (400 \text{ MeV})^2$ in quasielastic (e,e') scattering. EMA probably slightly underestimates the cross sections, but this mismatch will be investigated in the forthcoming weeks. Surprises at lower energies are possible.
- There is a Rosenbluth-like procedure based on detailed comparisons with DWBA calculations that insures an extraction of the longitudinal and transverse response functions even in heavy-weight nuclei like ^{208}Pb.

Additional comments and explanations

Slide 3 (Long range Coulomb force):

Since αZ is large, a first order correction in αZ for observables like e.g. scattering cross sections are not reliable.

Slide 4 (Quasielastic (e,e') scattering):

For large momentum transfer (photon virtuality), e.g. $Q^2 > (400\,\mathrm{MeV})^2$, the typical length scale for the virtual photon is of the order of 0.5 fm. When inclusive (e,e') scattering is modeled as knockout process of individual nucleons, the electron really has to get 'close' to the nucleon in order to knock it (out). Therefore, the knockout process has a quasilocal character and the photon line in the picture should be 'much shorter'.

Slide 5 (Quasielastic peak):

Naive calculation of the position of the quasielastic peak leads to $\omega_{Peak} \sim 100$ MeV for the kinematics/data shown on the slide. However, there is an additional shift of the peak due to the (average) binding energy of the nucleons (~ 25 MeV) AND due to the Coulomb distortion of the electron (additional 10 MeV).

One must point out that so-called 'exact' calculations of Coulomb corrections using a single particle shell model for the nucleus fail to reproduce the cross section for large energy transfer (where e.g. pion production sets in). It is therefore desirable to find a general strategy which allows to analyse the effect of the Coulomb distortion in experimental data (an EMA-like procedure). This procedure might then depend not too strongly on the details of the nuclear model.

Slide 7 (Eikonal approximation):

In an early attempt to calculate Coulomb corrections in inclusive (e,e') scattering, I used the eikonal approximation in conjunction with a focusing factor (slide 9) given basically by the central focusing value which is too large. This has a non-negligible impact on the size of the Coulomb corrections (see 'N.B.' on slide 9 and slide 22).

Slides 10/11 (Electron wave functions...):

Details how electron scattering states are constructed from the radial wave functions (which are obtained e.g. by numerical integration of the coupled differential equations) can be found in the literature. Slide 11 shows the enhanced electron amplitude inside a ^{208}Pb nucleus (with a radius of about $\sim$ 7 fm) on a plane which contains the nuclear center. The circle in the lower picture depicts the nuclear radius of 7 fm.

Slides 13/14/15 (Focusing):

The focusing in the center of the nucleus is indeed very well approximated by $(k - V(0))/k$ for high electron energies, but the average focusing is smaller (mainly due to the transverse decay of the focusing, slide 15). It can be calculated from an effective potential value $V_{\text{eff}} \sim 20$ MeV, whereas $V(0) \sim 25$ MeV. Also the average momentum of the electron in the nuclear region is well described by this effective value. The first order correction in αZ to the electron wave function (for a homogeneously charged sphere) provides indeed an inadequate description of the Coulomb distortion (mainly in transverse direction). Slides 14/15 show the focusing along straight lines through the center of the nucleus in direction of the electron momentum, and in transverse direction, respectively.

Slide 16 (Wave length modification):

For electron energies larger than 300 MeV, the eikonal approximation provides a very good description of the phase of the electron wave function in the nuclear region.

Slide 17 (Average focusing):
The average focusing description works also for charge and current densities constructed from different in- and out states (for high enough electron energies). Slide 18 gives a visualization of the transition charge density of an electron scattered by 60^o, with positive helicity in the initial and final state.

Slide 22 (Knoll operator):
The first picture shows the effective electron charge density in the nuclear region for plane waves. The focusing of the electron waves leads to an enhanced charge density (second picture). Applying the Knoll operator to the electron charge density leads to the charge density shown in the third picture - the profile looks asymmetric, however the total charge is again nearly exactly the same as in the plane wave case. The effective momentum transfer (photon propagator) cancels (approximately) the focusing effect this way.

Slide 23 (Eikonal and EMA):
The eikonal calculations published in Nucl. Phys. A were performed using the central focusing factor which is too large. The EMA calculations were also performed by using the central value for lead (25 MeV). The upper plot shows the ratio of cross sections calculated in plane wave Born approximation for electrons with the Coulomb corrected results in different approaches. Correcting the EMA calculations by naive linear interpolation corresponding to an effective potential value of 18.5 MeV towards the PWBA result and reducing the eikonal result by using a smaller focusing factor leads to the second plot: The EMA and improved eikonal results show now a very similar behavior. The plot hints

at the possibility that EMA slightly underestimates the cross sections by about 4% (Kinematics: initial electron energy 485 MeV, scattering angle 60^o).